PUBLICATIONS OF THE ASTRONOMICAL SOCIETY OF THE PACIFIC, **125**:1436–1442, 2013 December

Mg II h + k Flux—Rotational Period Correlation for G-type Stars

MANUEL OLMEDO, MIGUEL CHÁVEZ, EMANUELE BERTONE, AND VÍCTOR DE LA LUZ

Instituto Nacional de Astrofísica Optica y Electrónica Luis Enrique Erro#1, CP 72840, Tonatzintla, Puebla, Mexico;
olmedo@inaoep.mx, mchavez@inaoep.mx, ebertone@inaoep.mx, itztli@gmail.com

Received 2013 September 12; accepted 2013 October 07; published 2013 December 3

ABSTRACT. We present an analysis of the correlation between the mid-UV Mg II h and k emission lines and measured rotational periods of G-type stars. Based on IUE and HST high resolution spectra of a sample of 36 stars, we derive an exponential function that best represents the correlation. We find that the variation of the Mg II h + k fluxes is about a factor of 2.5 larger than that of Ca II H + K, indicating that the UV features are more sensitive to the decline of $P_{\rm rot}$. The comparison of UV-predicted rotational periods with those derived from empirical $P_{\rm rot}$ — Ca II H + K flux calibrations are consistent, with some scatter at large periods, where the emissions are less intense. We present newly derived rotational periods for 15 G-type stars.

Online material: color figures

1. INTRODUCTION

The rate at which main sequence stars rotate is certainly amongst the most fundamental stellar parameters. It has proven to be a fundamental tool in a variety of stellar astrophysical phenomena, in particular as a test of the dynamo theories. In the time domain, rotational periods are fundamental to understanding the evolution of angular momentum in low mass stars, from the T-Tauri stage to mature objects as our Sun. Additionally, rotational velocity has become a leading tool for determining stellar ages of main sequence stars in the field, for which other methods, such as the isochrone fitting, are difficult to apply (Soderblom 2010).

Direct measurements of the stellar rotational periods rely on the analysis of brightness variations on the stellar surface due to the presence of spots. Nevertheless, aside from highly magnetic objects of early-type where the spot coverage can be large, this method represents, in many instances, a difficult task for cooler stars. In G-type stars the flux fluctuation is rather weak and requires very long and precise photometric and spectroscopic observational programs. In order to cope with these potential constraints, other indirect methods have been implemented, mainly through the analysis of the rotationally driven chromospheric activity.

The correlation between the stellar chromospheric activity and rotation was first identified in the pioneering work of Kraft (1967). This relationship is generally explained by the balance between an enhanced magnetic field induced by rotation and the breaking due to loss of angular momentum by magnetized stellar winds (Mestel 1968). An additional part of the picture is given by the internal magnetic fields generated in the interiors of convective stars ($T_{\rm eff} < 8000$ K) through a solar-like dynamo mechanism.

Magnetic activity has been usually measured by the emission excess in the strong Ca II H and K features. The cardinal work initiated at Mount Wilson in the early sixties (Wilson 1963) was later continued through a number of extensive surveys (see, for instance, Duncan et al. 1991; Henry et al. 1996; Wright et al. 2004; Jenkins et al. 2008; Zhao et al. 2013).

Whilst the Ca II H and K lines have long been the workhorse for stellar activity studies, in particular due to their accessibility from ground based telescopes, the Mg II h and k emission lines in the mid-UV (2800 Å) has provided additional valuable diagnostics. These lines, with similar energetics to those of Ca II, present the advantage that their shallower absorption wings make the emission line easier to measure and less contaminated by the photosphere.

Early works on the Mg II h and k resonance lines by Hartmann et al. (1984) demonstrated that this chromospheric proxy strongly correlates with rotational period, $P_{\rm rot}$. Their study was based on a relatively small sample (31 objects) covering a wide range of mass and evolutionary status, and also included numerous binaries. More recently, Cardini & Cassatella (2007, hereafter CC07) analyzed a larger stellar sample and identified a loose correlation between Mg II flux and rotational period, a situation that is improved if age instead of rotational period is used.

In this paper, we revisit the Mg II h and k doublet as a powerful diagnostics of the rotational period of G-type stars by analyzing a stellar sample of main sequence and subgiant stars observed by International Ultraviolet Explorer (IUE), complemented with high resolution observations conducted by the Space Telescope Imaging Spectrograph (STIS) and the Goddard High Resolution Spectra (GHRS) on board the Hubble Space Telescope (HST). We calibrate the Mg II h and k absolute fluxes with measured rotational periods and apply the relation to

determine new rotational periods for 15 stars with high quality UV spectra.

2. THE STELLAR SAMPLE

The stellar sample upon which our analysis is based has been constructed from two different databases. The first is that of the IUE-Newly Extracted Spectra (INES[1]): We searched for all high resolution data available for objects in class 44 (G-type stars of luminosity classes IV and V). This search delivered nearly 500 spectra that were subsequently visually inspected to verify their quality. A total of 57 objects have been selected from this database. We have also searched available data on G-type stars from HST and found 19 objects: 17 are from STIS, 1 from GHRS, and 1 object has 1 image from both instruments. These data were taken from the HST-MAST archive[2] and StarCat (Ayres 2010). For the solar spectra, we extracted a high resolution spectrum of the Moon listed in class 02 of the INES archive.

The full sample consists of 75 object plus the Sun.[3] The stellar set is divided into three working subsamples. The first subsample consist of 37 stars (and the Sun) with rotational periods, that we call *primary*, and will be used to establish the calibration of the Mg II UV fluxes versus rotational period. For these objects, the rotational periods have been measured either through the analysis of the photometric modulation of the visible flux due to the uneven distribution of stellar spots on the stellar surface, or through variability of the Ca II emission. The data for these stars are given in Table 1 where columns 1–7 provide, respectively, the star name, the spectral type, the color index $B-V$, the effective temperature mainly obtained from the compilation of Soubiran et al. (2010), the calculated Mg II absolute flux (see next section), the rotational period, and a label of the reference for the period. The list of references is given at the bottom of the table. The second subsample is composed of 23 objects with *secondary* rotational periods, that is, periods determined through a calibration of Ca II emission and measured rotational periods. This dataset will serve as a test to compare rotational periods derived with our UV calibration with those computed from Ca II. Table 2 lists the objects included in this set. Column 1–5 are as in Table 1, while the last 3 columns provide the secondary rotational period, the reference for this period, and the rotational period estimated in this work, respectively. Finally, the third collection corresponds to 15 stars with no available information on their rotational periods, and for which we derive the first estimate of this parameter. This latter set is presented in Table 3, where we also provide our rotational periods and their estimated errors.

[1] Please see http://ines.ts.astro.it/cgi-ines/IUEdbsMY.

[2] Please see http://archive.stsci.edu/hst/.

[3] The complete set of images used in this work is listed in Table A.1 of Appendix A.

3. MEASURING THE $F_{\rm h+k}$

For the full stellar sample, we have adopted the process described in Hartmann et al. (1984) to measure the observed Mg II h and k fluxes $f_{\rm h+k}$ as the flux integral between the two minima in the h ($h1v$, $h1r$) and k ($k1v$, $k1r$) lines from the zero flux level (see Fig. 1). This process was conducted automatically, but verified (and corrected if needed) visually, in particular for stars with lower signal-to-noise ratios in these minima. This method differs from those implemented by Blanco et al. (1974), Linsky & Ayres (1978), and CC07 in that these works either include a correction for the photospheric contribution or perform the integration by considering a local continuum defined by the $k1$ and $h1$ minima. An alternative way to carry out the integration was provided by Buccino Mauas (2008), who considered a fixed 1.7 Å-width windows to calculate the flux in the k and h lines. In an ideal scenario one should eliminate the photospheric contribution by properly modeling the atmospheric absorption. Nevertheless, the space ultraviolet and in particular the Mg II features in the mid-UV still represent a challenge when modeling stellar atmospheres (see, e.g., Chavez et al. 2007). Additionally, it was argued by Hartmann et al. (1984) that the photospheric contribution in the Mg II lines is much less than for Ca II. Many objects have numerous spectra available, as many as 120 in the case of the star HD2151. For these objects we obtained the mean spectrum by weighting the available spectra by their quoted flux errors.

Observed integrated fluxes were then converted to absolute fluxes, $F_{\rm h+k}$, following the relation of Oranje et al. (1982):

$$\log(F_{\rm h+k}/f_{\rm h+k}) = 0.328 + 4\log T_{\rm eff} + 0.4(V + BC). \quad (1)$$

For each object we collected the V magnitudes from SIMBAD database, while the bolometric corrections were taken from Flower (1996). Effective temperatures are mainly from Soubiran et al. (2010) and, for a few objects, from Ammons et al. (2006). In the case of Sun, we have used the IUE spectrum of the Moon LWR09968HS, which was selected among the 21 available spectra, because of its high quality. For the purposes of treating this spectrum in a similar way as the rest of the stars, we have calculated $F_{\rm h+k}$ by adopting the V magnitude of the solar analog HD102365, a G2V star with stellar parameters very close to solar: $(T_{\rm eff}/\log g/[{\rm Fe/H}]) = (5637/4.45/-0.08)$ (Gratton et al. 1996). To obtain the error in the surface flux, we applied a Gaussian error propagation through equation (1). For the effective temperature we have used the errors provided in the Soubiran et al. (2010) and Ammons et al. (2006) catalogs; for stars with no quoted error in the catalogs, we adopted the mean uncertainty (95 K) of stars with temperature errors available. We assumed for V and BC the conservative values of 1% and 10% relative errors, respectively. The uncertainty on the observed flux $f_{\rm h+k}$ is obtained

TABLE 1
BASIC DATA FOR STARS WITH PRIMARY ROTATIONAL PERIODS.

Star	Spectral type	$B-V$	$T_{\rm eff}$ (K)	$\log F_{\rm h+k}$ (erg · s^{-1} cm^{-2})	$P_{\rm rot}$ (days)	Ref.
Sun	G2V	0.65	5775	6.02	26.09	D96
HD1835	G3V	0.67	5776	6.47	7.78	D96
HD9562	G1V	0.603	5849	5.68	29	B96
HD10700	G8.5V	0.72	5328	5.72	34	B96
HD11131	G1Vk:	0.632	5767	6.47	8.92	G00
HD13974	G0V	0.58	5606	6.29	11.1	SF87
HD20630	G5Vv	0.66	5696	6.50	9.24	D96
HD25680	G5V	0.62	5867	6.44	9.1	SF87
HD26756	G5V	0.706	5617	6.50	9.5	D84
HD26913	G8V	0.66	5616	6.55	7.15	D96
HD27406	G0V	0.572	6200	6.79	5.44	P03
HD28034	G0	0.555	6146	6.65	5.2	D84
HD28068	G1V	0.62	5758	6.64	7.73	P03
HD28205	G0	0.545	6244	6.58	6.7	D84
HD28344	G2V	0.619	5898	6.57	7.41	P03
HD28805	G5	0.755	5480	6.43	9.04	P03
HD30495	G1.5VCH-0.5	0.64	5836	6.51	11	B96
HD72905	G1.5Vb	0.58	5863	6.72	4.69	D96
HD73350	G5V	0.669	5779	6.44	6.14	G00
HD76151	G3V	0.67	5762	6.16	15	B96
HD95128	G1V	0.62	5869	5.74	22.7	S10
HD97334	G0V	0.61	5850	6.64	7.6	N84
HD101501	G8V	0.73	5450	6.29	16.68	D96
HD103095	G8Vp	0.75	5055	5.61	31	B96
HD114710	G0V	0.58	5963	6.34	12.35	D96
HD115383	G0V	0.59	6009	6.66	3.33	D96
HD115617	G7V	0.70	5558	5.81	29	B96
HD116956	G9V	0.81	5355	6.48	7.8	G00
HD117176	G5V	0.71	5530	5.55	31	H00
HD128987	G8Vk:	0.737	5557	6.49	9.35	G00
HD129333	G1.5V	0.59	5845	6.89	2.8	D96
HD142361	G3V	0.64	5175	6.90	1.06	M06
HD143761	G0V	0.60	5806	5.84	19	H00
HD152391	G8.5Vk:	0.76	5467	6.54	11.43	D96
HD182572	G8IV...	0.77	5595	5.85	41	B96
HD217014	G2.5IVa	0.70	5760	5.56	37	B96
HD283572	G5IV	0.81	4949	6.65	1.55	S09
HD131156A	G8V	0.777	5465	6.45	6.16	SF87

NOTE.—References.—(D96) Donahue et al. 1996; (B96) Baliunas et al. 1996; (P03) Pizzolato et al. 2003; (M06) Meyer et al. 2006; (D84) Duncan et al. 1984; (S10) Simpson et al. 2010; (SF87) Simon & Fekel 1987; (S09) Strassmeier 2009; (N84) Noyes et al. 1984; (H00) Henry et al. 2000; (G00) Gaidos et al. 2000

from the IUE and HST error vectors as a function of the wavelength; we added in quadrature the mean error in the intervals used to integrate each pair of Mg II lines. The latter is the main source of error on $F_{\rm h+k}$.

In order to test the consistency of our derived fluxes, in Figure 2 we compare our measurements of the Mg II k line flux with those reported by Cardini (2005) (for the 23 objects in common). Whilst the correlation is clear, our fluxes are higher by approximately 25% (about 0.1 dex) on average. This excess can be plausibly explained by the different integration processes. Since Cardini (2005) did not report the IUE images that were used, it is possible that they not coincide with ours, as may be the case of HD2151 for which our flux is 80% larger.

4. THE $F_{\rm h+k}$ — $P_{\rm rot}$ CORRELATION

In the upper panel of Figure 3 we plot $F_{\rm h+k}$ versus the rotational periods for the 38 objects (including the Sun) which have primary values for their rotational periods (Table 1). In this plot the different symbols stand for the origin of the data as indicated in the panel. All stars correspond to luminosity classes objects V except for the squared symbol that shows the location of the only luminosity class IV star. The starred symbol indicates the position of the Sun. We have attempted several functional forms to calculate the best fit and found that the function:

$$\log F_{\rm h+k} = A + Be^{\log P_{\rm rot}/C}. \quad (2)$$

TABLE 2
BASIC DATA FOR STARS WITH SECONDARY ROTATIONAL PERIODS.

Star	Spectral type	$B-V$	$T_{\rm eff}$ (K)	$F_{\rm h+k}$ (erg · s^{-1} cm^{-2})	$P_{\rm rot2}$ (days)	Ref.	$P_{\rm rot3}$ (days)	$\sigma_{P_{\rm rot3}}$ (days)
HD26923	G0IV	0.56	5986	6.58	7	B96	6.5	1.7
HD30649	G1V-VI	0.58	5791	5.92	17	W04	22.4	1.7
HD34411	G1.5IV-V	0.64	5821	5.61	24.26	S85	32.0	1.8
HD43587	G0V	0.59	5899	5.82	21.62	S85	25.3	1.7
HD52711	G4V	0.60	5891	5.82	18	W04	25.4	1.7
HD67228	G1IV	0.60	5738	5.45	27	W04	37.2	1.8
HD84737	G0.5Va	0.61	5894	5.89	27	W04	23.1	1.8
HD101563	G0V	0.66	5902	5.86	27	W04	24.0	1.7
HD102365	G2V	0.66	5575	5.81	24	SO97	25.7	1.7
HD104304	G8IV	0.78	5542	5.88	35	W04	23.5	1.7
HD109358	G0V	0.60	5901	5.91	16	W04	22.8	1.8
HD110897	G0V	0.50	5863	6.00	12.73	S85	20.1	1.7
HD120066	G0.5IV-V	0.66	5923	5.56	26	W04	33.7	1.8
HD144579	G8V	0.73	5301	5.67	34	W04	29.9	1.7
HD146233	G2Va	0.65	5785	5.84	24	W04	24.7	1.7
HD147513	G5V	0.60	5850	6.50	8.5	SO97	8.1	1.7
HD150706	G3V	0.57	5918	6.56	10.59	S85	6.8	1.9
HD157214	G0V	0.61	5675	5.86	29.84	S85	24.0	1.7
HD157347	G5IV	0.65	5677	5.86	30	W04	24.1	1.7
HD165185	G1V	0.57	5854	6.60	5.9	SO97	6.1	1.7
HD182488	G8V	0.79	5421	5.70	39	W04	29.1	1.8
HD188376	G5IV	0.75	5505	5.93	34	W04	22.1	1.7
HD188512	G9.5IV	0.85	5091	5.52	54	W04	35.1	1.8

NOTE.—References.—(B96) Baliunas et al. 1996; (SO97) Saar & Osten 1997; (S85) Soderblom 1985; (W04) Wright et al. 2004

where the coefficients $A = 7.125$, $B = -0.162$, $C = 0.674$, provided the lowest χ^2. The function is compatible with the exponential used in Noyes et al. (1984). However, as in Noyes et al. (1984), the adopted functional form does not have physical implications.

There is a relatively tight correlation for our sample of G-type stars, with much less dispersion than that observed in other works (e.g., Hartmann et al. 1984; Cardini & Cassatella 2007) that can be explained by the exclusion of the more active cool K and M-type stars. The lines in the plot correspond to the best fitted exponential function (*solid line*) and the $\pm 1\sigma$ levels (*dashed lines*).

Whilst at low rotational periods ($P_{\rm rot} < 4$ d) the diagram is less populated, the correlation indicates that for $P_{\rm rot} = 0$ the flux appears to reach a maximum of $\log F_{\rm h+k} \sim 6.8$. For periods larger than 4 days there is a decline of more than one decade. The three stars indicated with diamonds were not taken into account in the fitting calculation. The two with the lowest

TABLE 3
STARS WITH NEWLY DETERMINED ROTATIONAL PERIODS.

Star	Spectral type	$B-V$	$T_{\rm eff}$ (K)	$F_{\rm h+k}$ (erg · s^{-1} cm^{-2})	$P_{\rm rot3}$ (days)	$\sigma_{P_{\rm rot3}}$ (days)
HD2151	G0V	0.62	5773	5.76	27.1	1.7
HD16417	G1V	0.67	5797	5.82	25.2	1.7
HD20794	G8V	0.71	5430	5.80	25.9	1.7
HD44594	G1.5V	0.65	5799	5.96	21.2	1.7
HD59967	G3V	0.64	5780	6.56	7.00	1.7
HD76932	G2VFe-1.8CH	0.53	5849	5.94	21.9	1.7
HD136352	G4V	0.63	5623	5.78	26.7	1.7
HD181321	G2V	0.59	5816	6.63	5.7	1.7
HD184499	G0V	0.59	5723	5.98	20.7	1.7
HD190248	G8IV	0.76	5544	5.61	31.9	1.7
HD196378	G0VFe-0.8CH	0.51	6038	5.74	27.7	1.7
HD203244	G5V	0.73	5525	6.50	8.1	1.7
HD212330	G2IV-V	0.68	5650	5.50	35.8	1.8
HD212697	G3V	0.71	5769	6.82	2.7	1.9
HD225239	G2V	0.64	5593	5.90	22.9	1.7

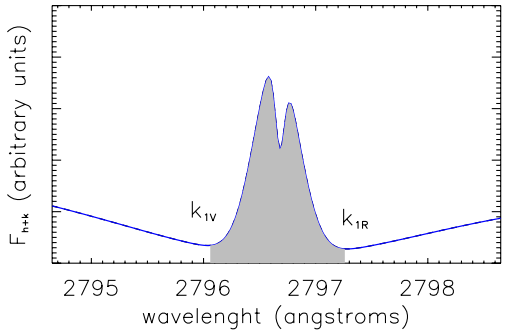

FIG. 1.—Synthetic profile of Mg II k line. The flux integration is made through the $k1v$ and $k1r$ minima limits. See the electronic edition of the *PASP* for a color version of this figure.

rotational periods correspond to pre-main sequence objects, whose inclusion would produce, in any case, negligible changes in the fitted function. The other object, which shows the largest deviation from the correlation depicted in Figure 3, is the metal-rich star HD182572. This a G8IV variable star whose rotational period of 41 days ($\log P_{\rm rot} = 1.61$; Baliunas et al. 1996) appears to be twice as large as predicted by its Mg II flux. Its measured rotational period is compatible with the period of ∼37 days estimated from the average rotational velocity ($v \sin i$) of 1.9 km s^{-1} in Glebocki & Gnacinski (2005) and the stellar radius of 1.38 $R_\odot$ (Boyajian et al. 2013). Variability can be a possible explanation for the discrepancy; however, Lockwood et al. (1997) found the root mean square of the brightness variation in Strömgren b and y bands to be just 0.0016 mag during a 12-year long interval (1984–1995). It is possible that an enhanced activity epoch around the IUE observation date (1979 December) produced such a strong

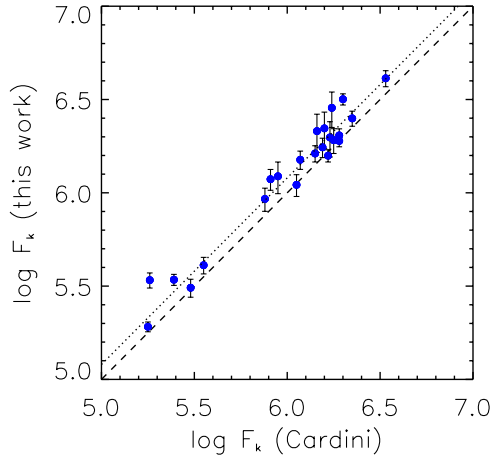

FIG. 2.—The absolute flux for the Mg II k line ($F_{\rm k}$) measured in this work vs. those of Cardini (2005). The *dashed line* is the one-to-one relation and the *dotted line* is a linear fit to the data. A similar procedure is used for the Mg II h line. See the electronic edition of the *PASP* for a color version of this figure.

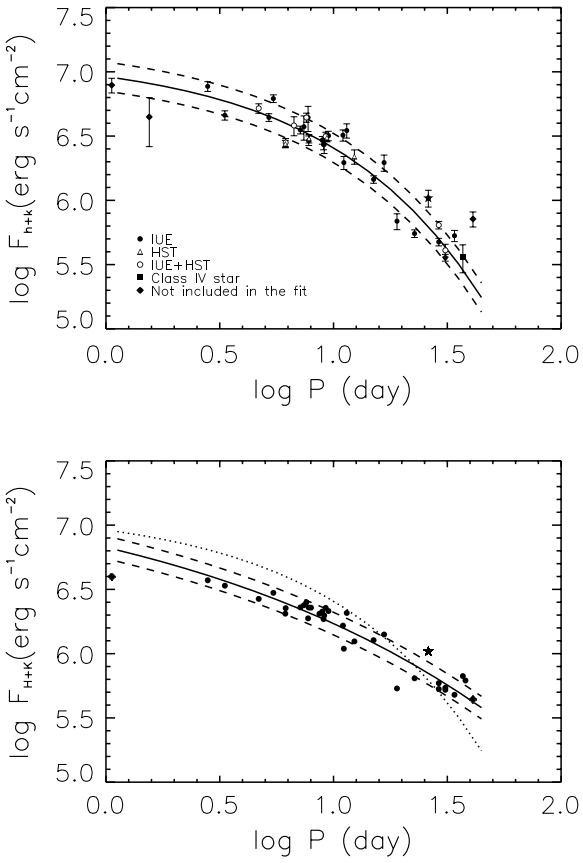

FIG. 3.—*Top panel*: Mean Mg II h + k flux ($F_{\rm h+k}$) as function of rotational period. *Solid circles*, *open circles*, and *open triangles* are mean $F_{\rm h+k}$ from IUE, HST, and HTS + IUE spectra, respectively. The sun is indicated with a star. The *solid line* is the best fit to the data, while the *dashed lines* indicate the ±1 sigma error. Diamonds are stars not used in the fit. *Bottom Panel*: Ca II H + K flux vs. rotational period, $F_{\rm H+K}$ derived from the $R_{\rm H+K}$ values given by Henry et al. (1996) and Wright et al. (2004). The *solid line* is the best fit using a similar exponential function as for UV data, shown as a *dotted line*.

UV flux, although this scenario might not be supported by the Ca II S-index monitoring by Duncan et al. (1991), unless the IUE observation actually coincided with a transient event.

An important aspect of the observed correlation of Mg II versus $P_{\rm rot}$ is the range of variation of $\log F_{\rm h+k}$. The difference between the highest and lowest values is 1.60 dex. In order to compare this difference with that to be expected from Ca II measurements, we have used the available $R_{\rm H+K}$ fluxes for the calcium line from Henry et al. (1996) and Wright et al. (2004) for the stars of our sample and transformed them into $F_{\rm H+K}$ by multiplying $R_{\rm H+K}$ by the bolometric luminosity σT^4, according to the definition of Noyes et al. (1984). We fit a similar function to equation (2) to the $F_{\rm H+K} - P_{\rm rot}$ values; this is shown in the lower panel of Figure 3, where the dotted line is the fit for Mg II case. Note that the variation of $F_{\rm H+K}$ is 1.20 dex, i.e., about 0.4 dex smaller than that for Mg II. We would like to remark that, had we included the star with the

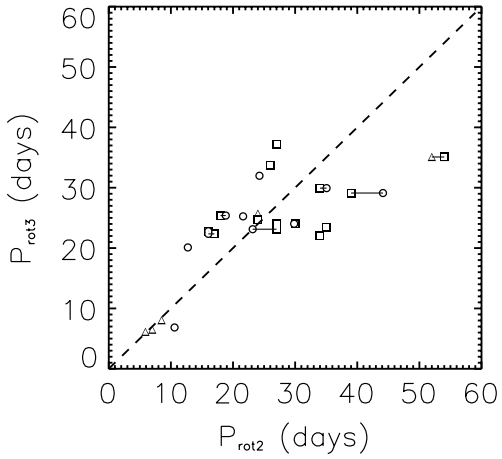

FIG. 4.—Comparison of calculated rotational periods ($P_{\rm rot3}$) and secondary rotational periods from literature ($P_{\rm rot2}$). Squares and circles have rotational periods from Wright et al. (2004) and Soderblom (1985), respectively; triangles are from Baliunas et al. (1996) or Saar & Osten (1997). Stars with periods from both groups are connected.

lowest rotational period (HD142361), the Ca II flux variation would have decreased to 1.09 dex due to the steeper correlation in the low period edge.

Another interesting feature of the panels depicted in Figure 3 is that the average standard deviation for both correlations are quite similar, with that of Mg II ($\sigma_{\rm h+k} \sim 0.11$ dex) slightly larger than for Ca II (~0.09 dex). In this regard, we have conducted a simple test to understand the extent to which the standard deviation can be ascribed to the $F_{\rm h+k}$ intrinsic variability of each star. For this purpose, we have compared the amplitude of the variation of the flux in the Mg II lines, $\Delta \log F_{\rm h+k}$, with $\sigma_{\rm h+k}$, for the 17 stars with multiple observations. The results of such a comparison indicate that $\Delta \log F_{\rm h+k} < \sigma_{\rm h+k}$ in 15 out of 17 cases. The main results of the analysis presented above demonstrates that the magnesium index is about 2.5 times more sensitive to rotational period than that of calcium.

5. NEW ROTATIONAL PERIODS

A direct application of the exponential fit obtained in the previous section is the determination of new rotational periods ($P_{\rm rot3}$) for the objects in Table 3. It is, however, important to compare UV derived periods with those determined from secondary methods, mainly through the calibration of the Ca II H and K lines. For this purpose we use the second stellar set in Table 2, for which we have collected calculated rotational periods from the literature: these secondary rotational periods ($P_{\rm rot2}$) are mainly from Soderblom (1985), Wright et al. (2004), and a few from Baliunas et al. (1996) and Saar & Osten (1997). In Figure 4 we illustrate the comparison of the Mg II vs Ca II rotational periods. The dashed line correspond to slope unity.

In general the points cluster around the one-to-one correlation with less agreement at large rotations periods ($P_{\rm rot} > 20$ d), hence for more mature stars with less intense chromospheric emission. The point that most deviates from the correlation is that for star HD188512 (β Aql, for which derived $P_{\rm rot} = 35.1$ d is significantly smaller than the Ca II derived periods in excess of 50 days). This star is a subgiant star which has 15 determinations of atmospheric parameters in the compilation of Soubiran et al. (2010). The effective temperatures for this object range from 4373 K to 5478 K, surface gravities from 1.3 dex to 3.79 dex, and a metallicity whose determinations vary nearly 0.6 dex. Even if we exclude the lowest gravity and highest temperature values (Luck & Heiter 2006; Luck & Lambert 1981),[4] this star has averaged parameters that are discrepant with the rest of the luminosity class IV stars in our sample, in particular for gravity. Being a more evolved star, the correlation given by equation (2) is most probably not applicable to this object.

For the stars in Table 3 we provide for the first time an estimation of their rotational period (column 6) and their uncertainties (column 7). Errors have been obtained through Gaussian propagation of errors of the fitting parameters of equation (2). Rotational periods for this sample span a wide range of values, from $P_{\rm rot} = 2.7$ d for HD212697 to 35.8d for HD212330. There are several objects with $P_{\rm rot}$ very similar to that of the Sun.

6. SUMMARY

We have measured the flux of the mid-UV emission lines Mg II h and k for 76 stars G-type stars (including the Sun) in the main sequence or in the subgiant branch. We used the 38 objects with a rotational period obtained from the periodic variability of their light curves to derive an analytical calibration of $F_{\rm h+k}$ vs. $P_{\rm rot}$. We found a tight correlation, which benefits from the inclusion of HST observations as they have a significantly better signal-to-noise ratio compared to the IUE spectra. This is the first time that HST UV data are used in the analysis of this relation, which we used to obtain the first estimates of the rotational periods for 15 stars with high quality mid-UV data.

Our results indicate that the Mg II h and k lines are about 2.5 times more sensitive to the rotational period than the frequently used chromospheric proxy of Ca II. The comparison of our UV-derived rotational periods with those obtained from similar correlations for Ca II shows a significant scatter for slow rotator, where perhaps the very faint Ca II H and K emission might be prone to large uncertainties.

[4] We would like to point out that there is a probable identification mismatch. According to Soubiran et al. (2010), the lowest value of log g for HD188512 has been compiled from Luck & Lambert (1981); however, this latter study is for supergiant stars, and the one with the reported parameters actually is β Aqr, a GOIb star.

APPENDIX A.

IDENTIFICATION OF IUE AND HST IMAGES

Table A1.

IMAGE IDENTIFICATION OF SOME OF THE SPECTRA USED IN THIS WORK. THE FULL LIST IS AVAILABLE UPON REQUEST FROM THE AUTHORS.

Star	Fits name
SUN	LWR09968HS_2790_2810
HD001835	LWP21832HL_2790_2810
	LWR11867HL_2790_2810
	LWP21823HL_2790_2810
	LWP14463HL_2790_2810
	LWR11851HL_2790_2810
	LWP24326HL_2790_2810
	LWP22038HL_2790_2810
	LWP22037HL_2790_2810
	LWP22005HL_2790_2810
	LWP22004HL_2790_2810
	LWP23657HL_2790_2810
HD009562	LWP02200HL_2790_2810
HD010700	LWR03702HL_2790_2810
	LWP04912HL_2790_2810
	LWR11587HL_2790_2810
	LWP02224HL_2790_2810
	LWR13817HL_2790_2810
	LWR04958HL_2790_2810
HD011131	LWP03613HL_2790_2810

REFERENCES

Ammons, S. M., Robinson, S. E., Strader, J., et al. 2006, ApJ, 638, 1004
Ayres, T. R. 2010, ApJS, 187, 149
Baliunas, S., Sokoloff, D., & Soon, W. 1996, ApJ, 457, L 99
Blanco, C., Catalano, S., Marilli, E., & Rodonò, M. 1974, A&A, 33, 257
Boyajian, T. S., von Braun, K., van Belle, G., et al. 2013, ApJ, 771, 40
Buccino, A. P., & Mauas, P. J. D. 2008, A&A, 483, 903
Cardini, D. 2005, A&A, 430, 303
Cardini, D., & Cassatella, A. 2007, ApJ, 666, 393
Chavez, M., Bertone, E., Buzzoni, A., et al. 2007, ApJ, 657, 1046
Donahue, R. A., Saar, S. H., & Baliunas, S. L. 1996, ApJ, 466, 384
Duncan, D. K., Frazer, J., Lanning, H. H., et al. 1984, PASP, 96, 707
Duncan, D. K., Vaughan, A. H., Wilson, O. C., et al. 1991, ApJS, 76, 383
Flower, P. J. 1996, ApJ, 469, 355
Gaidos, E. J., Henry, G. W., & Henry, S. M. 2000, AJ, 120, 1006
Glebocki, R., & Gnacinski, P. 2005, VizieR Online Data Catalog, 3244, 0
Gratton, R. G., Carretta, E., & Castelli, F. 1996, A&A, 314, 191
Hartmann, L., Baliunas, S. L., Noyes, R. W., & Duncan, D. K. 1984, ApJ, 279, 778
Henry, G. W., Baliunas, S. L., Donahue, R. A., Fekel, F. C., & Soon, W. 2000, ApJ, 531, 415
Henry, T. J., Soderblom, D. R., Donahue, R. A., & Baliunas, S. L. 1996, AJ, 111, 439
Jenkins, J. S., Jones, H. R. A., Pavlenko, Y., et al. 2008, A&A, 485, 571
Kraft, R. P. 1967, ApJ, 150, 551
Linsky, J. L., & Ayres, T. R. 1978, ApJ, 220, 619
Lockwood, G. W., Skiff, B. A., & Radick, R. R. 1997, ApJ, 485, 789
Luck, R. E., & Heiter, U. 2006, AJ, 131, 3069
Luck, R. E., & Lambert, D. L. 1981, ApJ, 245, 1018
Mestel, L. 1968, MNRAS, 138, 359
Meyer, M. R., Hillenbrand, L. A., Backman, D., et al. 2006, PASP, 118, 1690
Noyes, R. W., Hartmann, L. W., Baliunas, S. L., Duncan, D. K., & Vaughan, A. H. 1984, ApJ, 279, 763
Oranje, B. J., Zwaan, C., & Middelkoop, F. 1982, A&A, 110, 30
Pizzolato, N., Maggio, A., Micela, G., Sciortino, S., & Ventura, P. 2003, A&A, 397, 147
Saar, S. H., & Osten, R. A. 1997, MNRAS, 284, 803
Simon, T., & Fekel, F. C., Jr. 1987, ApJ, 316, 434
Simpson, E. K., Baliunas, S. L., Henry, G. W., & Watson, C. A. 2010, MNRAS, 408, 1666
Soderblom, D. R. 1985, AJ, 90, 2103
———. 2010, ARA&A, 48, 581
Soubiran, C., Le Campion, J.-F., Cayrel de Strobel, G., & Caillo, A. 2010, A&A, 515, A 111
Strassmeier, K. G. 2009, A&A Rev., 17, 251
Wilson, O. C. 1963, ApJ, 138, 832
Wright, J. T., Marcy, G. W., Butler, R. P., & Vogt, S. S. 2004, ApJS, 152, 261
Zhao, J. K., Oswalt, T. D., Zhao, G., et al. 2013, AJ, 145, 140